Supporting Information

A Fluorine-Enriched Gel Electrolyte with Universal Compatibility for Advanced Lithium Metal Batteries

Zunhao Fan[a‡], Qiao Zhang[b‡], Zengwu Wei[a], Li Liu[a], Danning Yu[a], Shuhao Liu[b], Kai Yu[b], Zoran Mandić[c], Kun Zheng[d], Hong Qiu[e], Renfang Wang[e], Mingjiong Zhou[a]*, Jun Wang[b]*, Xing Xin[a]*

[a] School of Material Science and Chemical Engineering, Ningbo University, Ningbo 315211, P. R. China.

[b] Guangdong Provincial Key Laboratory of Energy Materials for Electric Power, Department of Materials Science & Engineering School of Innovation and Entrepreneurship Southern University of Science and Technology, Shenzhen 518055, P. R. China.

[c] Faculty of Chemical Engineering and Technology, University of Zagreb, Trg Marka Marulića 19, 10000 Zagreb, Croatia.

[d] Faculty of Energy and Fuels AGH University of Krakow aleja Adama Mickiewicza 30, Krakow30-059, Poland.

[e] College of Big Data and software Engineering, Zhejiang Wanli University, Ningbo 315200, P. R. China.

‡ These authors contributed equally to this work (Z. Fan and Q. Zhang).

* Corresponding authors.

E-mail addresses: zhoumingjiong@nbu.edu.cn (M. Zhou); wangj9@sustech.edu.cn (J. Wang); xinxing@nbu.edu.cn (X. Xin).

1. Experiment section

1.1. Preparation of composite electrolyte

Polyethylene oxide (PEO), polytetrafluoroethylene (PTFE), polyvinylidene fluoride-co-hexafluoropropylene (PVDF-HFP) and polyvinylidene fluoride (PVDF) were mixed at a mass ratio of 3:3:3:1, and N-methyl-2-pyrrolidone (NMP) was added at a solvent-to-polymer mass ratio of 8:2. The mixture was stirred at room temperature for 36 h to obtain a homogeneous slurry. The resulting paste was then cast onto a PTFE plate and immersed in deionized water to induce phase inversion. The formed film was first dried in a blast oven at 40 °C for 24 h to obtain the composite fluorine-rich polymer matrix. Subsequently, different types of liquid electrolytes (LEs) were added to this matrix, leading to the formation of a fluorine-rich gel polymer electrolyte (denoted as CF-GPE), which were then punched into circular discs with a diameter of 19 mm for subsequent cell assembly.

1.2. Assembly of batteries

For the assembly of Li-O_2 batteries, Li foil was used as the anode, while the cathode was composed of carbon paper coated with 80 wt% multi-walled carbon nanotubes (MWCNTs). The CF-GPE was first placed on top of the Li foil, followed by dropwise addition of a liquid electrolyte (LE 160 μL) consisting of 1 M lithium bis(trifluoromethanesulfonyl)imide (LiTFSI) and 50 mM redox mediators (RMs, either LiBr or 2,2,6,6-tetramethylpiperidin-1-oxyl, TEMPO) dissolved in tetraethylene glycol dimethyl ether (TEGDME), allowing the system to undergo in situ gelation. Subsequently, the cathode sheet and a piece of nickel foam were assembled on top. The complete cell was then placed into a Swagelok-type Li–O_2 cell mold under a pure oxygen atmosphere. A commercial glass fiber (GF) separator was employed in the control samples for the Li–O_2 batteries.

For the assembly of Li||$LiCoO_2$ cells, $LiCoO_2$, Super P and PVDF were mixed at a weight ratio of

8:1:1 and dispersed in NMP. The slurry was stirred for 12 h and then cast onto aluminum foil to form a cathode film, which was subsequently vacuum dried at 110 °C for 12 h to obtain the cathode sheet. Lithium foil was used as the anode. During cell assembly, the CF-GPE was placed onto the cathode, followed by dropwise addition of the LE (160 μL), consisting of 1 M $LiPF_6$ in a 1:1 (v/v) mixture of ethylene carbonate (EC) and diethyl carbonate (DEC), with 5 vol% fluoroethylene carbonates (FEC) as an additive. A lithium foil, separator, stainless steel spacer, spring, and negative casing were then sequentially assembled, and the entire cell was sealed by pressing in a single step.

For the assembly of pouch cell, CF-GPE and $LiCoO_2$ cathodes were prepared as described above and cut to 4.3 cm × 5.6 cm. Lithium foil anodes were trimmed to the same dimensions. The cell stack was built by laminating, in sequence, the lithium-foil anode, the CF-GPE, and the $LiCoO_2$ cathode. The stack was pre-sealed inside an aluminum-laminated pouch, electrolyte was injected, and the cell was rested for 6 h. After vacuum sealing, the cell was rested for another 8 h. All operations were carried out in an Ar-filled glove box (H_2O and $O_2 < 0.01$ ppm).

1.3. Material Characterizations

The morphological characterization of the samples was performed using a Hitachi SU-70 field-emission scanning electron microscope (FESEM) equipped with an energy dispersive spectrometer (EDS), and a WMJ-9590 metallographic microscope. The functional group composition of the sample was investigated by Fourier Transform Infrared Spectrometer (FT-IR, Nicolet 6700). The surface species and chemical states of CF-GPE were studied by X-ray photoelectron spectroscopy (XPS) measurements (Thermo Scientific K-Alpha). The surface structure and phase composition were analyzed using a Bruker D8 Focus Advance X-ray diffractometer (XRD) equipped with Cu Kα radiation ($\lambda = 0.15406$ nm). After electrochemical cycling, the cells were disassembled inside an

argon-filled glove box to retrieve the cycled electrodes. The electrodes were subsequently rinsed with 1,2-dimethoxyethane (DME) to remove residual electrolyte and lithium salts. To prevent air exposure and oxidation, all the samples were stored and handled within the glove box prior to characterizations. All the measurements were carried out at ambient temperature.

1.4. Electrochemical measurements

Electrochemical impedance spectroscopy (EIS) was measured using a CHI660E electrochemical workstation. Ionic conductivity measurements were determined by analyzing assembled symmetrical cells consisting of stainless steel/separator/stainless steel, followed by dropwise addition of the LE (EC:DEC = 1:1 with 5 wt% FEC). The sweep frequency range was 1.0 MHz to 0.01 Hz with an amplitude of 5 mV. The conductivity calculation for different partitions follows Equation 1, where "d" represents the partition thickness, "S" corresponds to the electrode area, and "R" is the intrinsic resistance value obtained from EIS measurements [1].

$$\sigma = \frac{d}{R \times S} \tag{1}$$

The assembled symmetrical battery (Li||Li) was tested by chronoamperometry at 10 mV with an electrochemical workstation and the impedance values before and after the chronoamperometry were recorded to measure the Li^+ ion migration number (t_{Li^+}). The t_{Li^+} values with different electrolytes are calculated by Equation 2, where I_0 and I_{SS} are the initial current and steady-state current, respectively. R_0 and R_{SS} represent the resistance values before and after the disturbance, respectively [2].

$$t_{Li+} = \frac{I_{SS}(\Delta V - I_0 R_0)}{I_0(\Delta V - I_{SS} R_{SS})} \tag{2}$$

Exchange current density (i_0) was evaluated using cyclic voltammetry (CV) at a scan rate of 1.0 mV s^{-1} in the voltage range of –200 mV to 200 mV. To determine i_0, a linear fit was performed over

a voltage range of 80-120 mV, which facilitated the calculation of i_0 from the fitted Tafel plot. All charge/discharge measurements were performed by a LAND battery testing system (CTA2001A, Wuhan Land Electronics Co., Ltd.) at room temperature. For the Li||$LiCoO_2$ cells, the voltage window is 3.0 V to 4.2 V, and 1 C is equivalent to 270 mAh g^{-1}. The Li-O_2 cell tests were carried out at a current density of 100 mA g^{-1} with a fixed capacity of 500 mAh g^{-1}.

1.5. Differential electrochemical mass spectrometry (DEMS) analysis

DEMS was performed using a modified Swagelok-type Li-ion battery setup. The assembly features a cell equipped with two bonded polyetheretherketone tubes serving as gas inlet and outlet. The tubes were connected to a commercial quadrupole mass spectrometer (Hiden HPR-20) via a custom-made gas purge system. Gas flow adjustment was achieved using a flow meter (Linglu), with high-purity argon as the carrier gas and a controlled flow rate of 0.72 mL min^{-1}.

1.6. Molecular dynamics (MD) simulation

MD simulations were performed using Materials Studio with the following protocol: Initial atomistic models of polymer-electrolyte systems (PEO or PVDF-HFP chain with more than 3 repeat units solvated in 1M $LiPF_6$/EC:DEC (1:1 v/v) + 2 wt% FEC were constructed via the Amorphous Cell module under periodic boundary conditions (~1500 atoms; box size ~40 Å). The COMPASSII force field was applied after density calibration to experimental ranges (1.25–1.30 g/cm^3). Systems sequentially underwent: energy minimization using the Smart Minimizer algorithm with convergence criteria of 1.0 kcal/mol·(energy) and 0.5 kcal/mol·Å (force); followed by constant-pressure, constant-temperature (NPT) annealing (Berendsen barostat, 1 bar) comprising linear heating from 300 K to 500 K over 10 ps, a 5-ps isothermal hold at 500 K, and linear cooling to 300 K over 10 ps; subsequently canonical ensemble (NVT) equilibration at 300 K (Andersen thermostat) for 2 ns with a 1-fs timestep; and finally production MD under NVT at 300 K for 5 ns. Trajectories from the final 4 ns were analyzed to calculate Li^+ diffusion coefficients via the Einstein relation from mean square displacement (MSD)

and characterize microstructure through radial distribution functions (RDFs) and coordination numbers. The Li^+ self-diffusion coefficient D_{Li+} was calculated via the Einstein relation from the mean square displacement (MSD) using Equation 3 [3], where "t" denotes time, "N" represents the number of particles, and "r_i" indicates the position.

$$D_{Li^+} = \frac{1}{6N_{Li^+}} lim_{t \to \infty} \frac{d}{dt} \sum_{i=1}^{N_{Li^+}} \langle |r_i(t) - r_i(0)|^2 \rangle \quad (3)$$

2. Supplementary table

Table S1. Coordination numbers of Li^+ for CF-GPE, PEO and PVDF-HFP calculated by MD.

	Li-F (PF_6^-)	Li-O (EC)	Li-O (DEC)
CF-GPE	2	2.02	——
PEO	1.06	2.38	0.18
PVDF-HFP	1.12	2.81	0.25

3. Supplementary figures

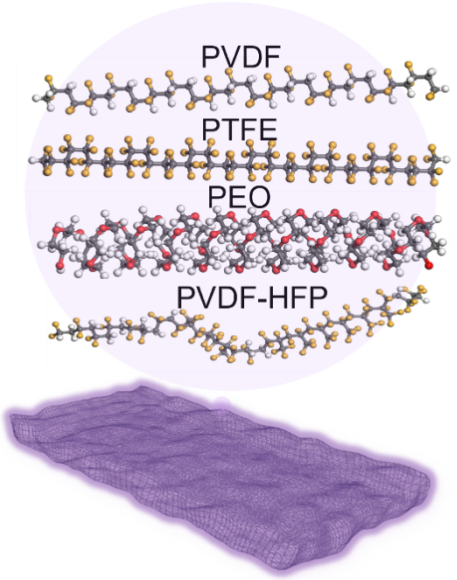

Fig. S1. Schematic structures of PVDF, PTFE, PEO and PVDF-HFP.

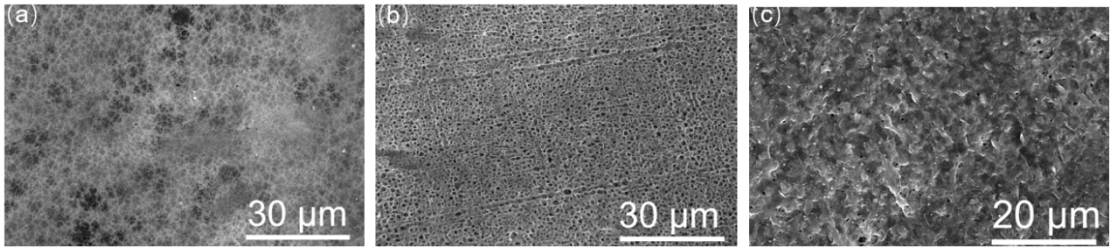

Fig. S2. SEM images of (a) PVDF, (b) PVDF-HFP and (c) CF-GPE without PVDF.

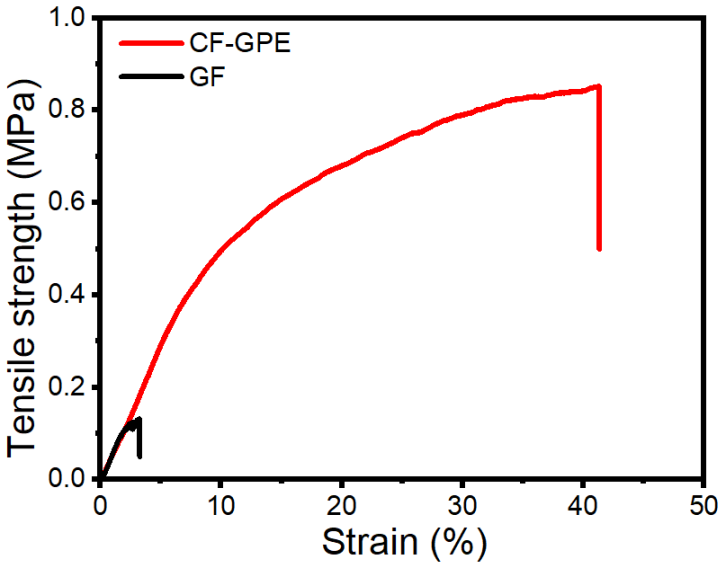

Fig. S3. Stress-strain curves of CF-GPE and GF.

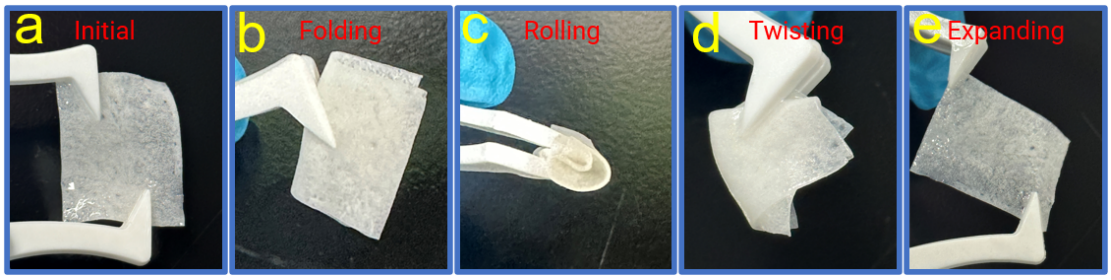

Fig. S4. Optical images of CF-GPE after (a) initialization, (b) folding, (c) winding, (d) twisting and (e) unfolding.

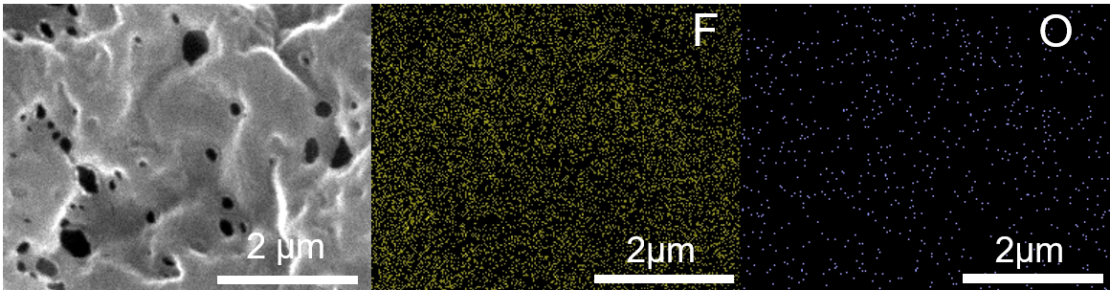

Fig. S5. SEM image and corresponding EDS mappings of CF-GPE membrane.

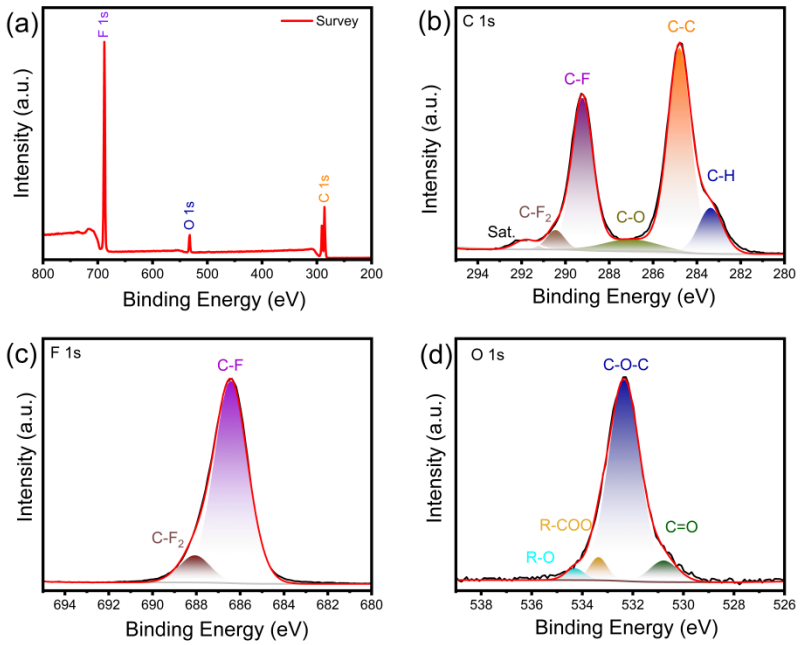

Fig. S6. (a) XPS survey spectrum and high-resolution spectra of C 1s (b), F 1s (c), and O 1s (d) for CF-GPE.

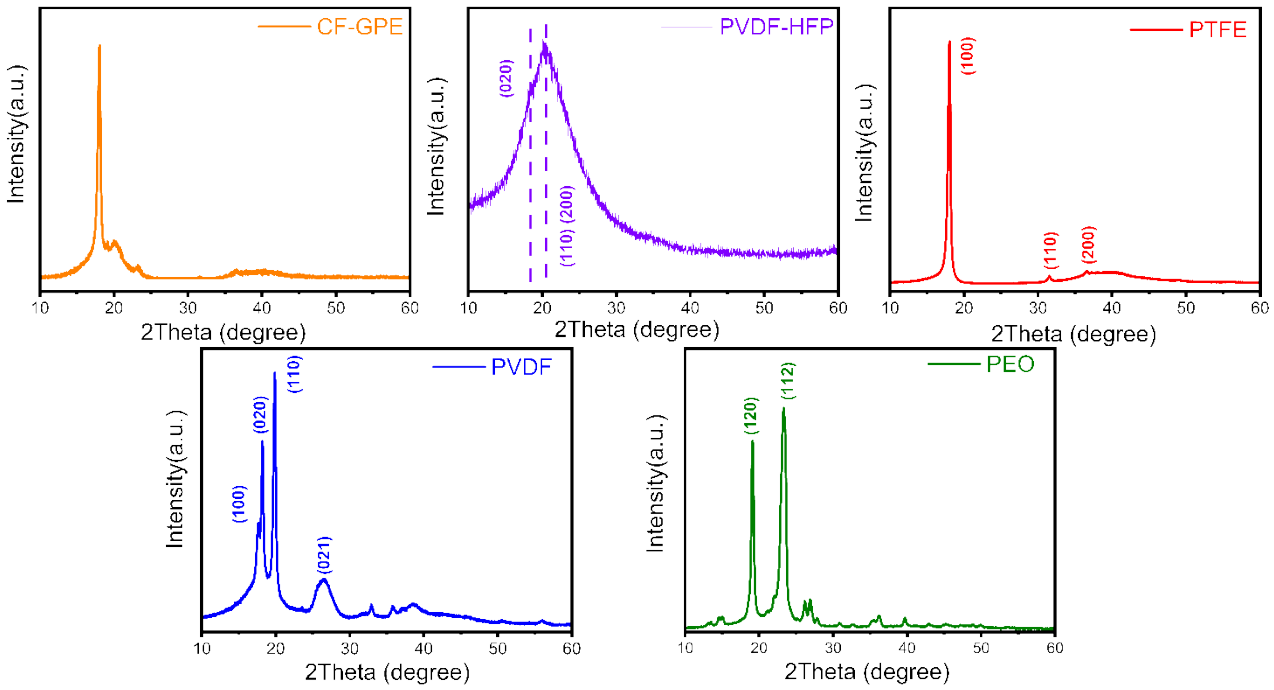

Fig. S7. XRD patterns of CF-GPE, PEO, PTFE, PVDF and PVDF-HFP.

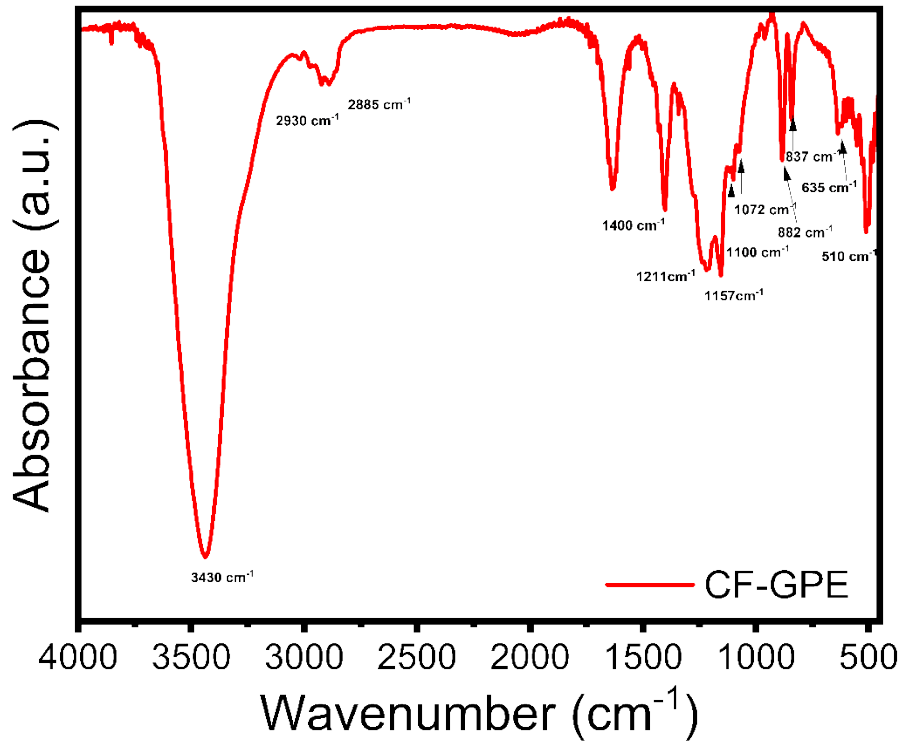

Fig. S8. FT-IR spectrum of CF-GPE.

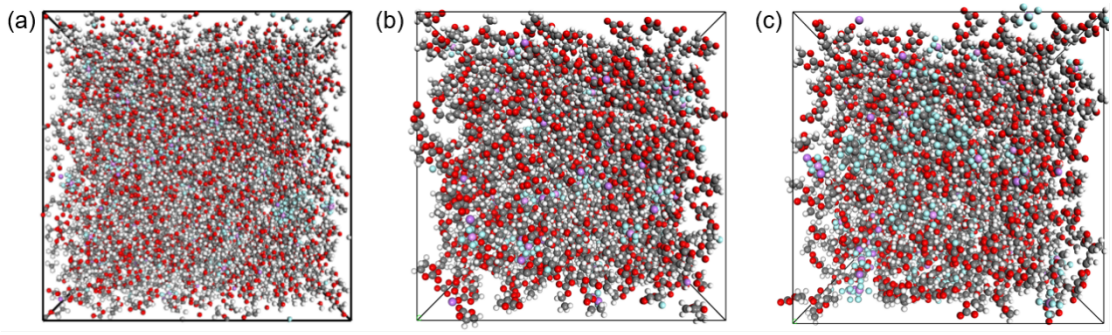

Fig. S9. Snapshots of MD simulated trajectories for (a) CF-GPE, (b) PEO and (c) PVDF-HFP.

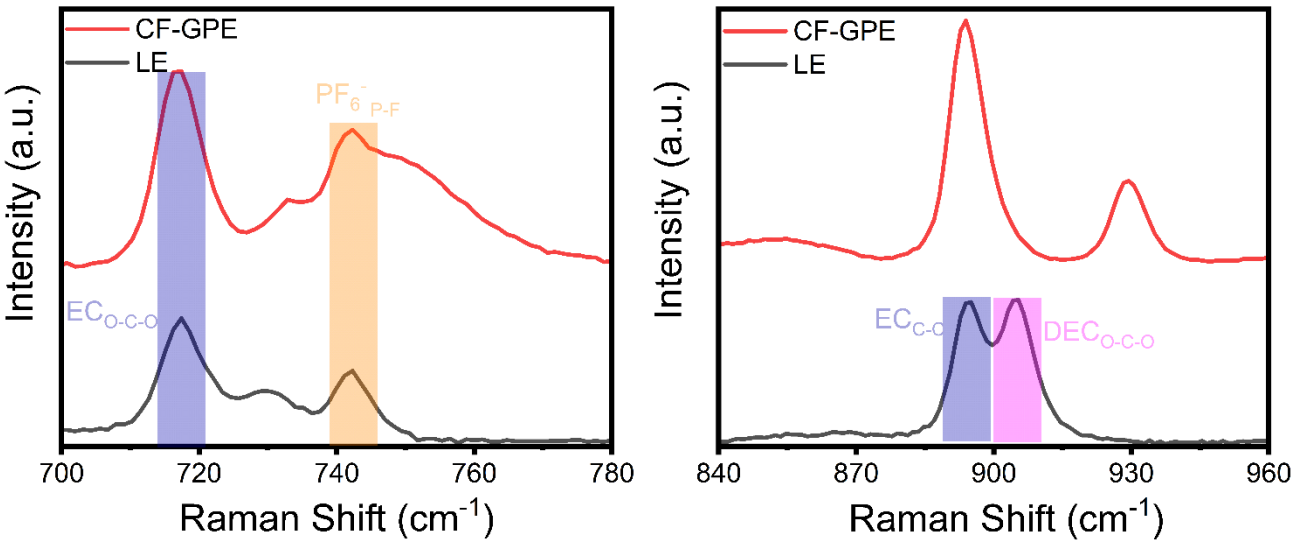

Fig. S10. Raman spectra of CF-GPE and LE in the ranges of 700–780 cm^{-1} and 840–960 cm^{-1}, respectively.

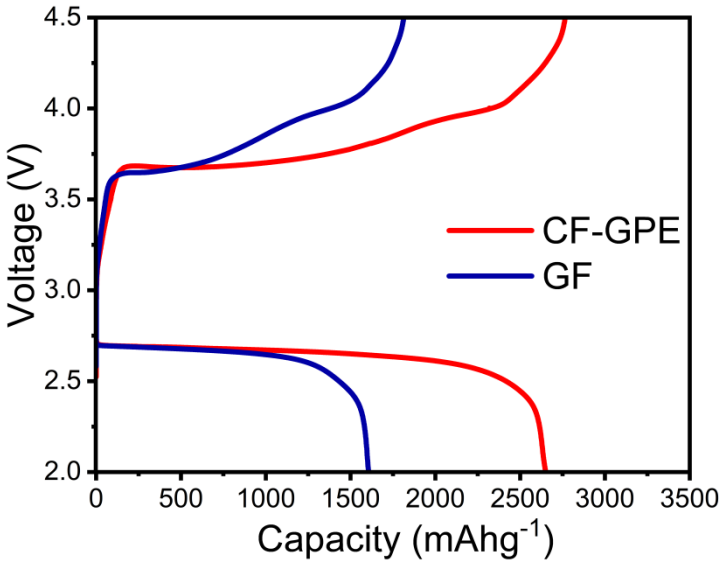

Fig. S11. Charge/discharge curves of Li-O_2 batteries assembled with CF-GPE and GF at 100 mA g^{-1}.

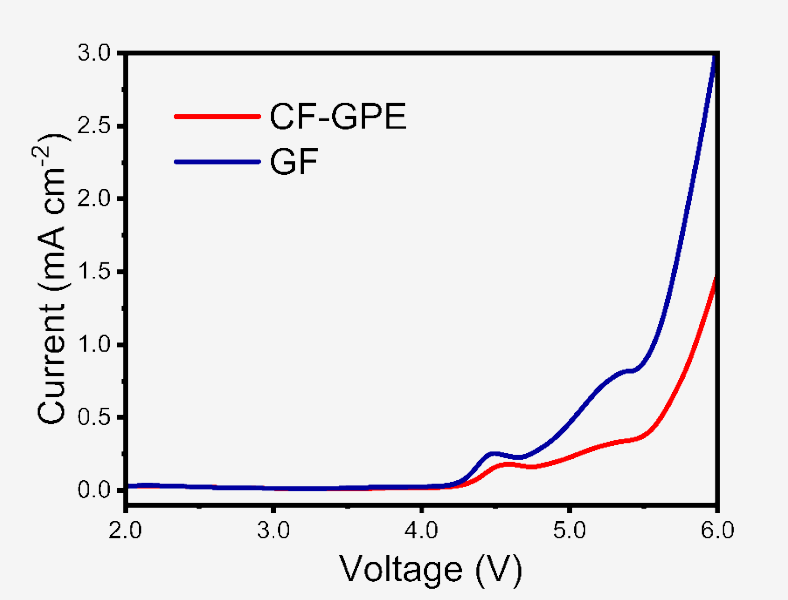

Fig. S12 LSV curves of CF-GPE and GF.

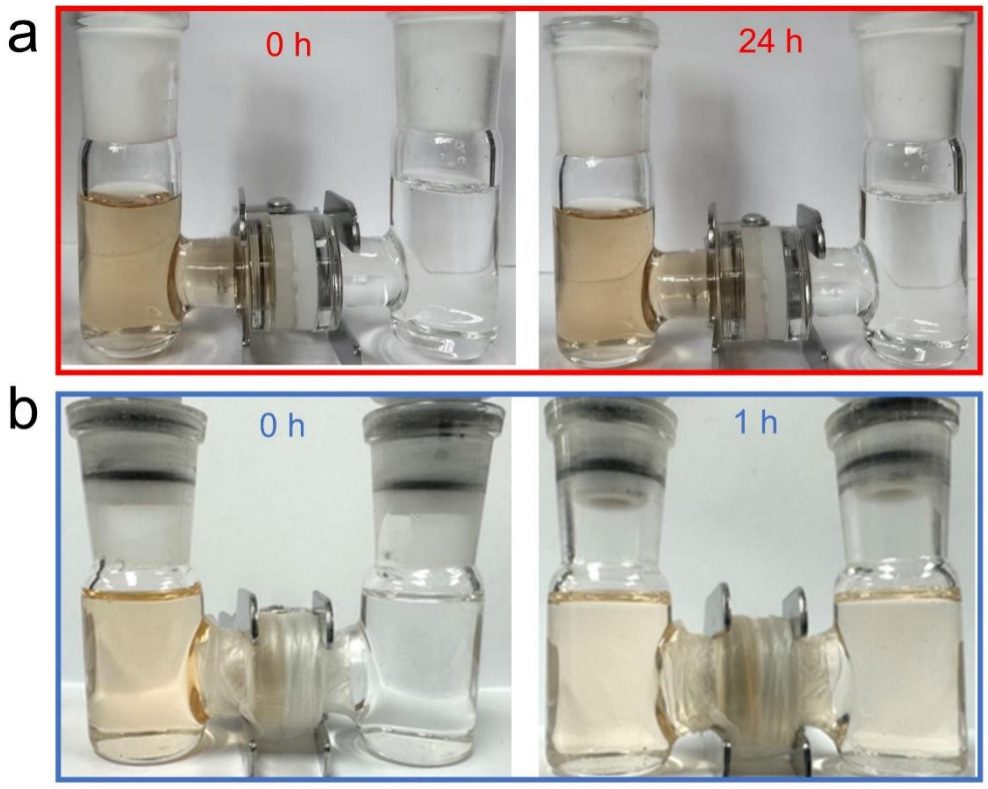

Fig. S13. U-type tube crossover experiments using (a) CF-GPE and (b) GF.

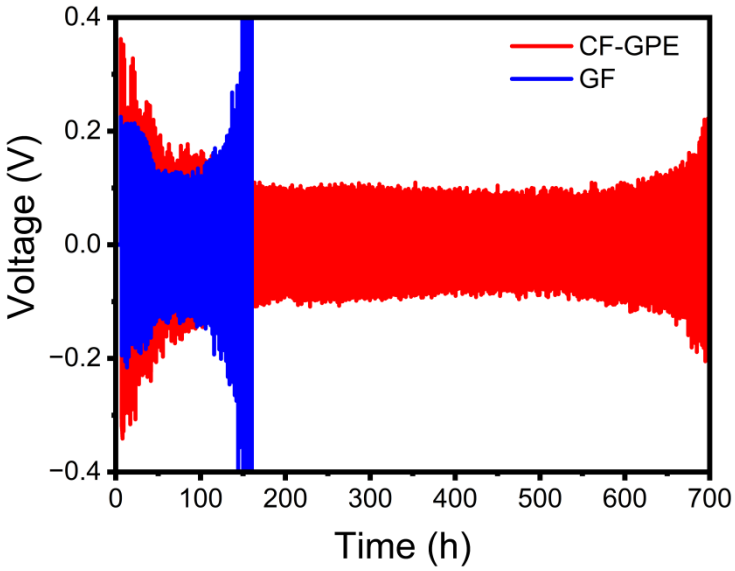

Fig. S14. Stripping/platting curves of Li||Li symmetric cells with CF-GPE and GF without RMs in 1 M LiTFSI/TEGDME electrolyte at 0.5 mA cm^{-2} and a fixed capacity of 0.5 mA h cm^{-2}.

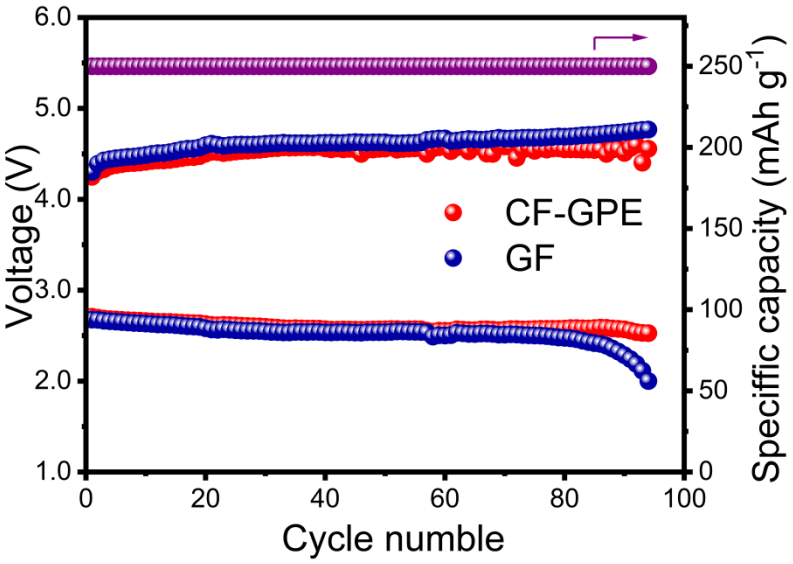

Fig. S15. Cycle performance of Li-O_2 batteries with CF-GPE and GF without RMs at 100 mA·g^{-1} and a limited capacity of 250 mAh g^{-1}.

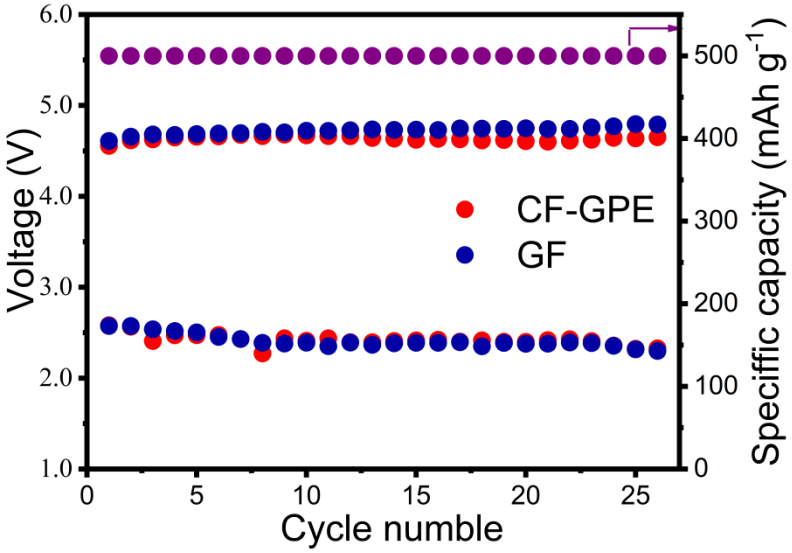

Fig. S16. Cycle performance of Li-O_2 batteries with CF-GPE and GF without RMs at 100 mA·g^{-1} and a limited capacity of 500 mAh g^{-1}

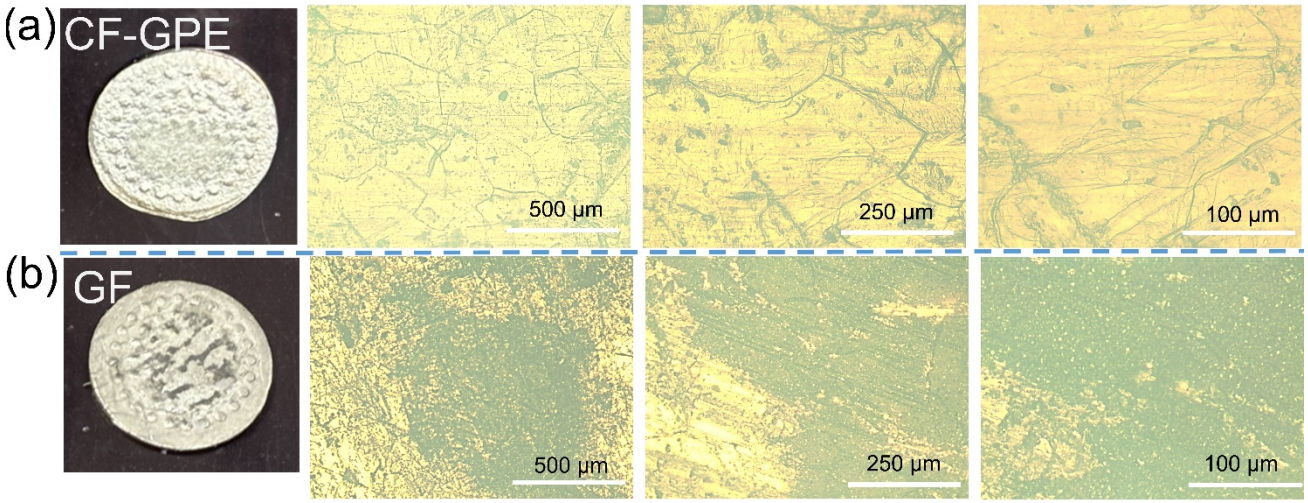

Fig. S17. Optical images and metallographic microscope images of Li foils in Li-O_2 batteries with GF (a) and CF-GPE (b) after exposing to air for 15 min.

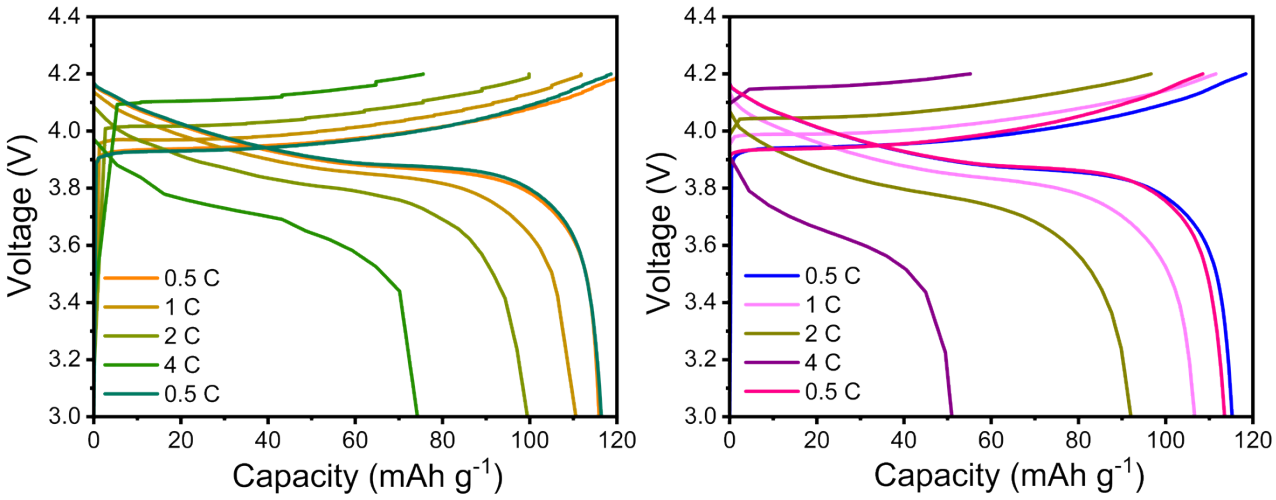

Fig. S18. Charge/discharge curves of Li||$LiCoO_2$ cells with CF-GPE (a) and LE (b) at various C rates.

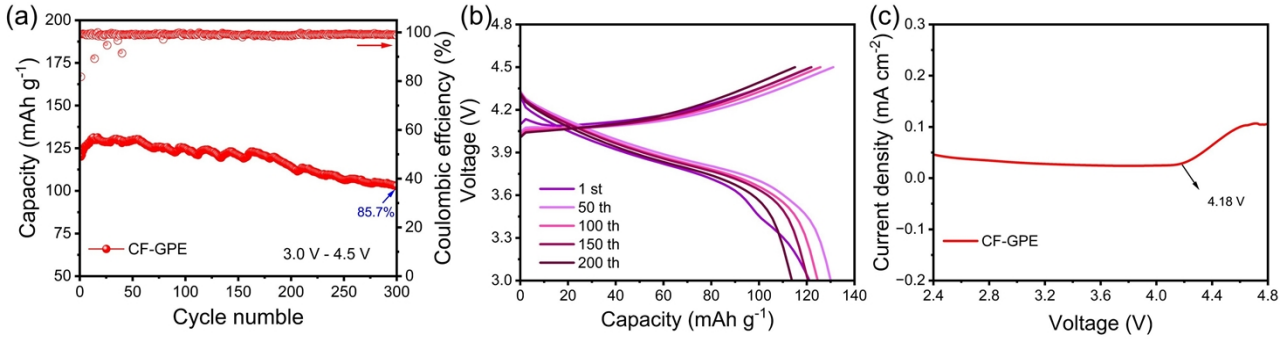

Fig. S19. Electrochemical performance test at a 4.5 V cutoff voltage

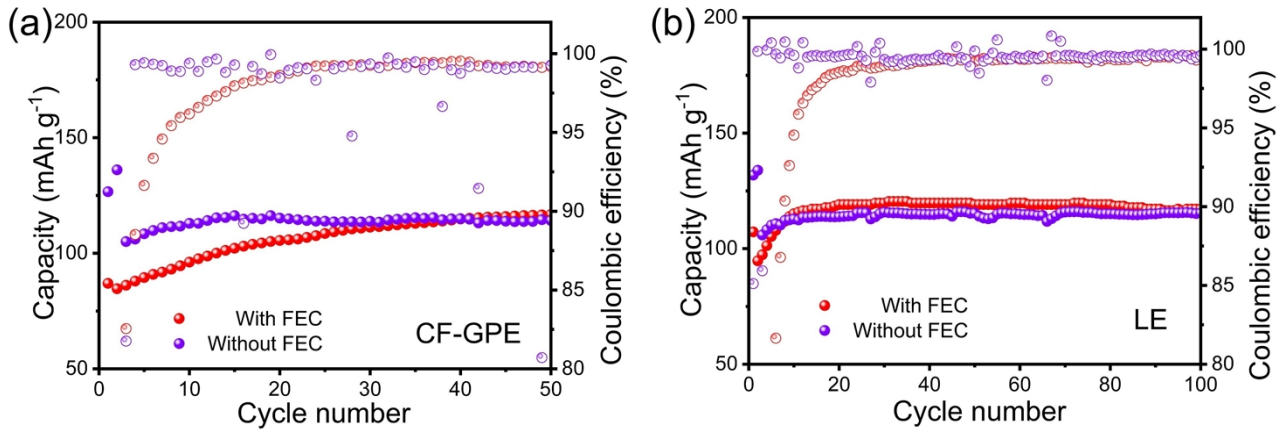

Fig. S20. Comparison of electrochemical performance with and without FEC.

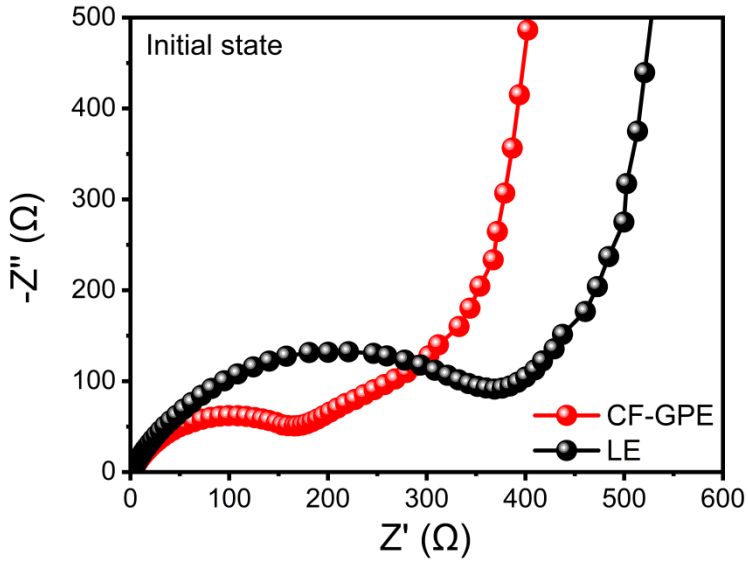

Fig. S21. Nyquist plots of Li||$LiCoO_2$ cells with CF-GPE and LE at initial state.

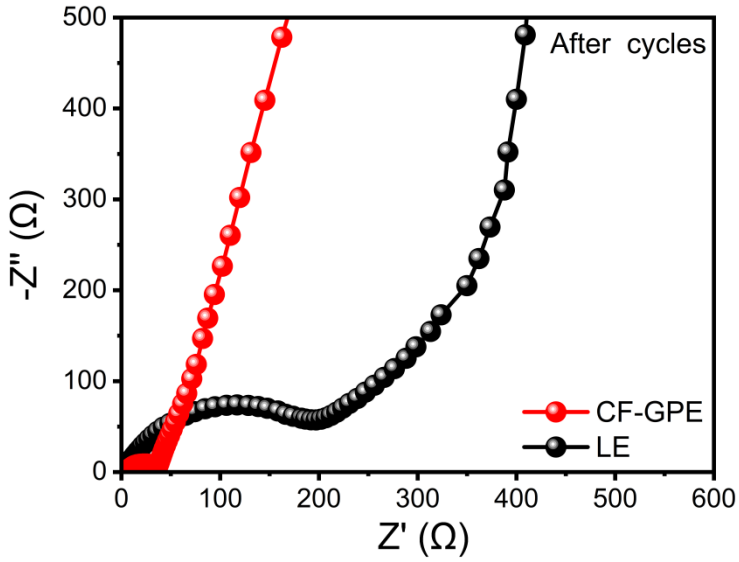

Fig. S22. Nyquist plots of Li||$LiCoO_2$ cells with CF-GPE and liquid electrolyte after 100 cycles.

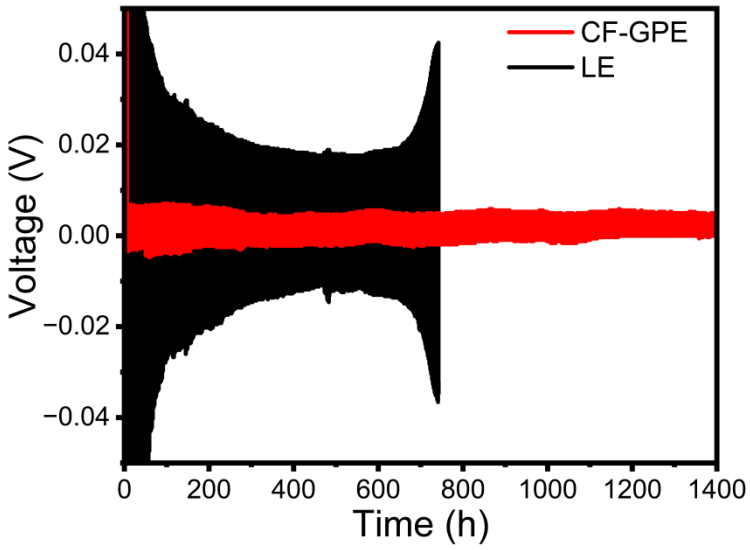

Fig. S23. Stripping/plating plots of Li||Li symmetric cells with CF-GPE and LE under a pressure of 250 kPa.

References

[1] J.S. Park, J.H. Choi, J.J. Woo, S.H. Moon, An electrical impedance spectroscopic (EIS) study on transport characteristics of ion-exchange membrane systems, *J. Colloid Interface Sci.,* 2006, **300**, 655-662.

[2] J. Evans, C.A. Vincent, P.G. Bruce, Electrochemical measurement of transference numbers in polymer electrolytes, *Polymer,* 1987, **28**, 2324-2328.

[3] A. Einstein, Über die von der molekularkinetischen Theorie der Wärme geforderte Bewegung von in ruhenden Flüssigkeiten suspendierten Teilchen, *Ann. Phys*. 2006, **322**, 549-560.